Tuan, Hoang Duong, Ngo, Duy Trong, Tam, Ho Huu Minh. “Joint power allocation for MIMO-OFDM communication with full-duplex relaying.” Published in Proceedings of the 2016 10th International Conference on Signal Processing and Communication Systems (ICSPCS 2016). (2016)

Available from: http://dx.doi.org/10.1109/ICSPCS.2016.7843374

Joint Power Allocation for MIMO-OFDM Communication with Full-Duplex Relaying

Hoang Duong Tuan*, Duy Trong Ngo†, and Ho Huu Minh Tam*
*Faculty of Engineering and Information Technology, University of Technology Sydney, Australia
(email: tuan.hoang@uts.edu.au, huuminhtam.ho@student.uts.edu.au)
†School of Electrical Engineering and Computer Science, The University of Newcastle, Australia
(email: duy.ngo@newcastle.edu.au)

***Abstract*—We address the problem of joint power allocation in a two-hop MIMO-OFDM link where a source node sends data to a destination node via an amplify-and-forward relay. Since the relay operates in the full-duplex mode, it receives and forwards data simultaneously. Our design objective is to maximize the end-to-end throughput, subject to either the joint sum-power constraint of both the source and the relay or the individual sum-power constraints at the source and the relay. The formulated problems are large-scale nonconvex optimization problems, for which efficient and optimal solutions are not available. Using the successive convex optimization approach, we develop a novel iterative algorithm of extremely low complexity that is especially suitable for large-scale computation. In each iteration, a simple closed-form solution is derived for the approximated convex program. The proposed algorithm is proved to always converge to at least a local optimum of the original nonconvex problems. Numerical results confirm that the devised algorithm converges quickly, and that our optimal power allocation solutions help realize the potential throughput gain of MIMO-OFDM full-duplex relaying over the conventional half-duplex relaying strategy.**

I. Introduction

The fifth-generation (5G) wireless networks target a $1,000$-fold increase in the network capacity to meet the ever growing user demands for high-speed and ubiquitous network access. Multiple-input multiple-output (MIMO) communications and cooperative orthogonal frequency division multiplexing (OFDM) relaying techniques play a key role in supporting such an ambitious objective. MIMO transmission and reception increase the channel capacity through spatial multiplexing, modulation and coding. Cooperative relaying provides greater coverage without deploying costly additional base stations.

OFDM relays are traditionally designed for the half-duplexing (HD) mode, where signal transmission and reception take place in different time slots and/or frequency bands. Only after fully receiving a data packet, the HD relay nodes forward it to the destination. On the other hand, full-duplexing (FD) has recently been proposed as one of the key transceiver techniques for 5G networks with the hope of doubling the spectral efficiency [1], [2]. The end-to-end delay is significantly reduced with simultaneous signal transmission and reception in the same time slot and on the same frequency band at the FD relay node. However, such bidirectional communication on the same radio resource block was assumed technically impossible, due to the large self-interference (SI) caused by the transmit antenna to the receive antenna on the same device. Recent advances in hardware design have suppressed the SI to a level potentially suitable for practical FD applications [3]–[5].

Finding efficient power allocations to realize the potential gains of the MIMO-OFDM FD relaying strategy remains an open research topic. Such allocations are still under-developed even for the conventional MIMO-OFDM HD relaying networks. In [6], the problem of power allocation for amplify-and-forward (AF) HD relays is investigated to maximize the instantaneous sum throughput. Since the objective function is not jointly but separately concave in the source and relay power variables, [6] proposes alternating optimization at the source and at the relay with individual per-node power constraints.

For the joint sum-power constraint at both source and relay, [6] resorts to a high signal-to-noise ratio (SNR) approximation for the throughput to become a jointly concave function in the source and relay power variables [7, Prop. 1 and Appendix B]. Although a closed-form optimal solution is available for the convex reformulation, such an approximation at high SNR regions does not always hold in practice. OFDM subchannels tend to be assigned with very different transmit power levels. Good subchannels are typically allocated more power to achieve high SNRs while unfavorable subchannels may even get zero SNRs. With the high SNR approximation of [6], the original nonconvex program is transformed to an *inequivalent* optimization problem. Upper bound maximization is given by [6], [7] for the original nonconvex maximization, where lower bound maximization should always be naturally preferred. In general, the solutions found by either alternating optimization or convex relaxation may not even satisfy the Karush-Kuhn-Tucker (KKT) necessary conditions for optimality.

It is even more challenging to find efficient power allocations for a MIMO-OFDM two-hop network with FD relaying. Such a highly nonconvex problem is unlikely to be solved via only one convex relaxation as in [6], [7]. To the best of our knowledge, there exists no efficient computational solution that guarantees optimality for this problem. In this paper, we develop a new iterative algorithm of extremely low computational complexity to jointly allocate the transmit power at the source and the relay. We tackle the nonconvex optimization problem via solving a sequence of convex programs in the complete set of source and relay power variables. The proposed approach applies equally well to both joint and separate sum-power constraints.

Our convex approximations are far from trivial even in the simplest scenario of MIMO-OFDM HD relaying considered in [6]. With the new bounding technique, the devised algorithm is novel even from an optimization-theoretical perspective. As

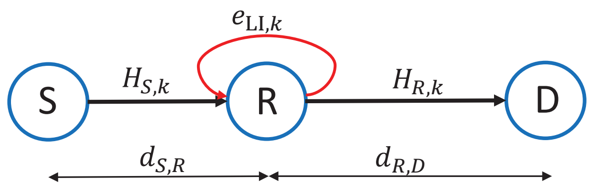

Fig. 1. A two-hop network with one source node (S), one full-duplex relay node (R) and one destination node (D)

each iteration of the algorithm always yields an improved solution, it is guaranteed to converge to at least a local optimum of the original nonconvex problems. Importantly, unlike [8], [9] we derive a simple closed-form solution for the convex program in each iteration, which requires extremely low computational complexity. Our algorithm is therefore particularly suitable for large-scale computation. Numerical results show that our efficient power allocation scheme markedly enhances the throughput of the FD relaying over the HD relaying strategy in the low SI regions.

Notation. Boldfaced symbols are used for optimization variables whereas non-boldfaced symbols for deterministic terms, regardless of whether they are matrix, vector or scalar. The dimensions of these symbols are interpreted from context, and should there be any ambiguity they will be explicitly specified.

II. System Model and Problem Formulations

Consider a two-hop relaying network as shown in Fig. 1. Using K OFDM subcarriers, the N_S-antenna source node S sends data information to the N_D-antenna destination node D with the help of an N_R-antenna AF FD relay node R. For simplicity and without loss of generality, let us assume that $N_S = N_D = N_R = N$. Denote the set of OFDM subcarriers as $\mathcal{K} \triangleq \{1, \ldots, K\}$. We assume there is no direct link between the two nodes S and D, e.g., building structures prevent signal penetration. The channel impulse response is assumed to be time-invariant during the time for exchanging information. Furthermore, full channel state information is made available at the nodes by some high-performing channel estimation mechanism in place. A central processing unit is employed to collect all the channel state information from the nodes (via either wireline or wireless links), perform the network optimization and disseminate the computational solution back to the nodes.

Data symbol $s_k \in \mathbb{C}^N$ from node S is linearly precoded before transmitting on subcarrier $k \in \mathcal{K}$ as $\tilde{s}_k = \Psi_k s_k$, where $\Psi_k \in \mathbb{C}^{N\times N}$ is the transmit precoding matrix on subcarrier k by node S. The received vector symbol on subcarrier k at node R is

$$y_{R,k} = H_{S,k}\tilde{s}_k + e_{\mathrm{LI},k} + \tilde{w}_{R,k}, \tag{1}$$

where $H_{S,k} \in \mathbb{C}^{N\times N}$ is the MIMO channel matrix between node S and node R on subcarrier k; $e_{\mathrm{LI},k} \in \mathbb{C}^N$ is the relay FD loop interference on subcarrier k; and $\tilde{w}_{R,k} \in \mathbb{C}^N$ is additive zero-mean Gaussian noise with covariance $\mathcal{R}_R$ encompassing all OFDM impairments such as intercarrier power leakage, narrow band interferences, channel estimation error and baseband noise [10]–[12].

Node R then multiplies $y_{R,k}$ by a matrix F_k and broadcasts the processed signal vector to node D. The received signal vector at node D is expressed as:

$$\begin{aligned}\tilde{y}_{D,k} &= H_{R,k}F_k\left(H_{S,k}\tilde{s}_k + e_{\mathrm{LI},k} + \tilde{w}_{R,k}\right) + \tilde{w}_{D,k}\\ &= \underbrace{H_{R,k}F_kH_{S,k}\Psi_k s_k}_{\text{desired signal}} + \underbrace{H_{R,k}F_k e_{\mathrm{LI},k}}_{\text{amplified FD relay loop interference}}\\ &\quad + \underbrace{H_{R,k}F_k\tilde{w}_{R,k}}_{\text{amplified relay noise}} + \tilde{w}_{D,k},\end{aligned} \tag{2}$$

where $H_{R,k} \in \mathbb{C}^{N\times N}$ is the MIMO channel matrix between node R and node D on subcarrier k; and $\tilde{w}_{D,k}$ is the zero-mean Gaussian noise at node D with covariance $\mathcal{R}_D$ encompassing all impairments such as intercarrier power leakage, narrow band interferences, channel estimation error and baseband noise [10]–[12].

Without loss of generality, we assume that $H_{S,k}$ and $H_{R,k}$ are nonsingular. They can thus be represented by the singular value decomposition (SVD) as:

$$H_{S,k} = V_{S,k}\Lambda_{S,k}U_{S,k} \quad \text{and} \quad H_{R,k} = U_{R,k}\Lambda_{R,k}V_{R,k} \tag{3}$$

with unitary matrices $U_{t,k}$ and $V_{t,k}$, $t \in \{S, R\}$ and diagonal matrices $\Lambda_{t,k} = \text{diag}\left\{\sqrt{h_{t,k,n}}\right\}_{n=1}^N$, $t \in \{S, R\}$. By taking

$$\begin{aligned}F_k &= V_{R,k}^H\bar{\mathbf{\Lambda}}_k V_{S,k}^H,\ \ \bar{\mathbf{\Lambda}}_k = \text{diag}\left\{\sqrt{\beta_{k,n}}\sqrt{\mathbf{p}_{R,k,n}}\right\}_{n=1}^N;\\ \Psi_k &= U_{S,k}^{-1}\check{\mathbf{\Lambda}}_k,\ \ \check{\mathbf{\Lambda}}_k = \text{diag}\left\{\sqrt{\mathbf{p}_{S,k,n}}\right\}_{n=1}^N,\end{aligned} \tag{4}$$

one can rewrite (2) as:

$$\begin{aligned}y_{D,k} &= \underbrace{\Lambda_{R,k}\bar{\mathbf{\Lambda}}_k\Lambda_{S,k}\check{\mathbf{\Lambda}}_k s_k}_{\text{desired signal}} + \underbrace{\Lambda_{R,k}\bar{\mathbf{\Lambda}}_k t_{\mathrm{LI},k}}_{\text{FD loop interference}} + \underbrace{\Lambda_{R,k}\bar{\mathbf{\Lambda}}_k w_{R,k}}_{\text{amplified relay noise}}\\ &\quad + w_{D,k},\end{aligned} \tag{5}$$

where

$$\begin{aligned}y_{D,k} &= U_{R,k}^{-1}\tilde{y}_{D,k}, \quad t_{\mathrm{LI},k} = V_{S,k}^H e_{\mathrm{LI},k},\\ w_{R,k} &= V_{S,k}^H\tilde{w}_{R,k}, \quad w_{D,k} = U_{R,k}^{-1}\tilde{w}_{D,k}.\end{aligned} \tag{6}$$

The noises $w_{R,k}$ and $w_{D,k}$ are still zero-mean Gaussian with covariances

$$\mathcal{R}_{R,k} = V_{S,k}^H\mathcal{R}_R V_{S,k} \text{ and } \mathcal{R}_{D,k} = U_{R,k}^{-1}\mathcal{R}_D U_{R,k}^{-H}, \tag{7}$$

respectively. With (5), we have shown that the FD relay MIMO channel in each OFDM subcarrier can be diagonalized into N parallel channels.

In (4), $\mathbf{p}_{S,k,n}$ and $\mathbf{p}_{R,k,n}$ are respectively the equivalent transmit power of node S to node R and that of node R to node D on spatial channel n in subcarrier k. Note that while the relaying power in F_k is not amplified, the gain $\beta_{k,n}$ ensures that the transmit power of each channel n on subcarrier k is indeed $\mathbf{p}_{R,k,n}$. In regard to the self-loop interferences in (6), it follows from [4] and [13] that practically $\mathcal{E}\{||t_{\mathrm{LI},k}||^2\} \le h_{\mathrm{LI}}\sum_{n=1}^N \mathbf{p}_{R,k,n}$ for some instantaneous residual self-loop interference power h_{LI}. To have mathematically tractable formulations for power allocation, we make the following simplified assumption [7]:

$$\mathcal{E}\{|t_{\mathrm{LI},k}(n)|^2\} \le h_{\mathrm{LI},k,n}\mathbf{p}_{R,k,n}, \tag{8}$$

where $h_{\mathsf{LI},k,n}$ represents the instantaneous residual self-loop interference power of spatial channel n on subcarrier k at node R. It follows that the amplify gain $\beta_{k,n}$ in (4) is:

$$\begin{aligned}\beta_{k,n} &= \sqrt{\frac{1}{h_{S,k,n}\mathbf{p}_{S,k,n} + h_{\mathsf{LI},k,n}\mathbf{p}_{R,k,n} + \mathcal{R}_{R,k}(n,n)}} \\ &= \sqrt{\frac{1/\mathcal{R}_{R,k}(n,n)\left(\gamma_{\mathsf{LI},k,n}\mathbf{p}_{R,k,n}+1\right)}{\bar{h}_{S,k,n}\gamma_{k,n}(\mathbf{p}_{S,k,n},\mathbf{p}_{R,k,n})+1}},\end{aligned} \tag{9}$$

where we define $\gamma_{\mathsf{LI},k,n} \triangleq h_{\mathsf{LI},k,n}/\mathcal{R}_{R,k}(n,n)$, $\bar{h}_{S,k,n} \triangleq h_{S,k,n}/\mathcal{R}_{R,k}(n,n)$ and

$$\gamma_{k,n}(\mathbf{p}_{S,k,n},\mathbf{p}_{R,k,n}) \triangleq \frac{\mathbf{p}_{S,k,n}}{\gamma_{\mathsf{LI},k,n}\mathbf{p}_{R,k,n}+1}. \tag{10}$$

The signal-to-noise ratio (SNR) at node D on spatial channel n of subcarrier k is then expressed as:

$$\mathrm{SNR}_{k,n} = \frac{\bar{h}_{S,k,n}\gamma(\mathbf{p}_{S,k,n},\mathbf{p}_{R,k,n})\left(h_{R,k,n}/\mathcal{R}_{D,k}(n,n)\right)\mathbf{p}_{R,k,n}}{1+\bar{h}_{S,k,n}\gamma(\mathbf{p}_{S,k,n},\mathbf{p}_{R,k,n}) + \left(h_{R,k,n}/\mathcal{R}_{D,k}(n,n)\right)\mathbf{p}_{R,k,n}}. \tag{11}$$

Upon defining

$$\begin{gathered} a_{(k-1)N+n} \triangleq \bar{h}_{S,k,n},\ b_{(k-1)N+n} \triangleq h_{R,k,n}/\mathcal{R}_{D,k}(n,n), \\ \gamma_{\mathsf{LI},(k-1)N+n} \triangleq \gamma_{\mathsf{LI},k,n}, \\ \mathbf{x}_{(k-1)N+n} \triangleq \mathbf{p}_{S,k,n},\ \mathbf{y}_{(k-1)N+n} \triangleq \mathbf{p}_{R,k,n}, \\ \gamma_{(k-1)N+n}(\mathbf{x}_{(k-1)N+n},\mathbf{y}_{(k-1)N+n}) \triangleq \gamma_{k,n}(\mathbf{p}_{S,k,n},\mathbf{p}_{R,k,n}), \\ \mathbf{x} \triangleq (\mathbf{x}_1,\ldots,\mathbf{x}_{KN})^T,\ \mathbf{y} \triangleq (\mathbf{y}_1,\ldots,\mathbf{y}_{KN})^T,\ M \triangleq KN, \end{gathered}$$

we are concerned with the problem of maximizing the instantaneous end-to-end throughput under transmit power constraints. Such an optimization problem is formulated as:

$$\max_{(\mathbf{x},\mathbf{y})} \sum_{i=1}^{M} \ln\left(1+\frac{a_i\gamma(\mathbf{x}_i,\mathbf{y}_i)b_i\mathbf{y}_i}{1+a_i\gamma(\mathbf{x}_i,\mathbf{y}_i)+b_i\mathbf{y}_i}\right) \tag{12}$$

subject to the joint sum-power constraint

$$\sum_{i=1}^{M}(\mathbf{x}_i+\mathbf{y}_i) \le P, \tag{13}$$

or the separate sum-power constraints

$$\sum_{i=1}^{M}\mathbf{x}_i \le P_1, \quad \sum_{i=1}^{M}\mathbf{y}_i \le P_2. \tag{14}$$

Here, $P, P_1, P_2 \ge 0$ are predefined power budgets. In practice, the users and the relay have separate power supplies constrained by (14) and the power allocation is performed at individual nodes. However, it is also important to consider the joint power allocation with the joint sum-power constraint (13) to gain meaningful insights into the power utilization of the system, and thereby realizing its full capacity.

III. Proposed Jointly Optimal Power Allocation

For the ease of reference, we present below the mathematical properties that are frequently used in our solution development.

- **(P1)**: $\ln(x_1+x_2) \le \ln\left(x_1^{(0)}+x_2^{(0)}\right) + \frac{1}{x_1^{(0)}+x_2^{(0)}}\left[\left(x_1-x_1^{(0)}\right)+\left(x_2-x_2^{(0)}\right)\right]$ for all $x_1>0, x_2\ge 0, x_1^{(0)}>0, x_2^{(0)}\ge 0$.
- **(P2)**: $\ln(x_1+x_2) \ge \ln\left(x_1^{(0)}+x_2^{(0)}\right) + \frac{1}{x_1^{(0)}+x_2^{(0)}}\left[x_1^{(0)}\left(\ln x_1 - \ln x_1^{(0)}\right) + x_2^{(0)}\left(\ln x_2 - \ln x_2^{(0)}\right)\right]$ for all $x_1>0, x_2>0, x_1^{(0)}>0, x_2^{(0)}>0$.

Property **(P1)** follows from the concavity of function $h(x_1,x_2) \triangleq \ln(x_1+x_2)$ while Property **(P2)** from the convexity of function $\tilde{h}(\tilde{x}_1,\tilde{x}_2) \triangleq \ln\left(e^{\tilde{x}_1}+e^{\tilde{x}_2}\right)$ is convex in $(\tilde{x}_1,\tilde{x}_2)$. The latter is the key for the success of the SCALE algorithm in the multiuser OFDM spectrum balancing problem [14].

For our problems of interest (12) s.t. (13)/(14), the cross term $\gamma(\mathbf{x}_i,\mathbf{y}_i)\mathbf{y}_i$ in the objective function contributes greatly to their computational difficulty. Fortunately, we can separate these variables without any loss of accuracy. Let us define:

$$\begin{aligned} f_i(\mathbf{x}_i,\mathbf{y}_i) &\triangleq \ln(1+a_i\mathbf{x}_i+\gamma_{\mathsf{LI},i}\mathbf{y}_i)+\ln(1+b_i\mathbf{y}_i), \\ g_i(\mathbf{x}_i,\mathbf{y}_i) &\triangleq \ln\left(1+a_i\mathbf{x}_i+(b_i+\gamma_{\mathsf{LI},i})\mathbf{y}_i+\gamma_{\mathsf{LI},i}b_i\mathbf{y}_i^2\right)\end{aligned}$$

for $i=1,\ldots,M$. We then rewrite (12) as:

$$\begin{aligned} F(\mathbf{x},\mathbf{y}) &= \sum_{i=1}^{M}[\ln(1+a_i\gamma(\mathbf{x}_i,\mathbf{y}_i))+\ln(1+b_i\mathbf{y}_i) \\ &\qquad -\ln(1+a_i\gamma(\mathbf{x}_i,\mathbf{y}_i)+b_i\mathbf{y}_i)] \\ &= \sum_{i=1}^{M}[\ln(1+a_i\mathbf{x}_i+\gamma_{\mathsf{LI},i}\mathbf{y}_i)+\ln(1+b_i\mathbf{y}_i) \\ &\qquad -\ln\left(1+a_i\mathbf{x}_i+(b_i+\gamma_{\mathsf{LI},i})\mathbf{y}_i+\gamma_{\mathsf{LI},i}b_i\mathbf{y}_i^2\right)] \\ &\triangleq f(\mathbf{x},\mathbf{y})-g(\mathbf{x},\mathbf{y}), \end{aligned} \tag{15}$$

where

$$f(\mathbf{x},\mathbf{y}) \triangleq \sum_{i=1}^{M} f_i(\mathbf{x}_i,\mathbf{y}_i) \tag{16}$$

is concave, and

$$g(\mathbf{x},\mathbf{y}) \triangleq \sum_{i=1}^{M} g_i(\mathbf{x}_i,\mathbf{y}_i) \tag{17}$$

is neither concave nor convex. Problems (12) s.t. (13)/(14) now become:

$$\max_{(\mathbf{x},\mathbf{y})} F(\mathbf{x},\mathbf{y}) = f(\mathbf{x},\mathbf{y})-g(\mathbf{x},\mathbf{y}) \quad \text{s.t.} \quad (13)/(14). \tag{18}$$

Following the iterative d.c. (difference of two convex functions) optimization method [8], [15], [16], we seek a global convex upper bound for $g(\mathbf{x},\mathbf{y})$, which agrees with $g(\cdot)$ at a given point $\left(x^{(\kappa)},y^{(\kappa)}\right)$.

By property **(P1)**, we have that

$$\begin{aligned} &g_i(\mathbf{x}_i,\mathbf{y}_i) \\ &\le g_i(x_i^{(\kappa)},y_i^{(\kappa)}) + c_i^{(\kappa)}\left[\left(a_i\mathbf{x}_i+(b_i+\gamma_{\mathsf{LI},i})\mathbf{y}_i+\gamma_{\mathsf{LI},i}b_i\mathbf{y}_i^2\right)\right. \\ &\quad \left.-\left(a_ix_i^{(\kappa)}+(b_i+\gamma_{\mathsf{LI},i})y_i^{(\kappa)}+\gamma_{\mathsf{LI},i}b_i(y_i^{(\kappa)})^2\right)\right], \end{aligned}$$

for all $\mathbf{x}_i\ge 0, \mathbf{y}_i \ge 0, x_i^{(\kappa)}\ge 0, y_i^{(\kappa)} \ge 0$ and where

$$c_i^{(\kappa)} = \frac{1}{1+a_ix_i^{(\kappa)}+(b_i+\gamma_{\mathsf{LI},i})y_i^{(\kappa)}+\gamma_{\mathsf{LI},i}b_i(y_i^{(\kappa)})^2}. \tag{19}$$

Then, the convex quadratic function $g^{(\kappa)}(\mathbf{x},\mathbf{y})$ defined by

$$\begin{aligned}
&g^{(\kappa)}(\mathbf{x},\mathbf{y}) \\
&\triangleq g(x^{(\kappa)},y^{(\kappa)})+\sum_{i=1}^{M} c_i^{(\kappa)}\left(a_i\mathbf{x}_i+(b_i+\gamma_{\mathsf{LI},i})\mathbf{y}_i+\gamma_{\mathsf{LI},i}b_i\mathbf{y}_i^2\right) \\
&\quad -\sum_{i=1}^{M} c_i^{(\kappa)}\left(a_i x_i^{(\kappa)}+(b_i+\gamma_{\mathsf{LI},i})y_i^{(\kappa)}+\gamma_{\mathsf{LI},i}b_i(y_i^{(\kappa)})^2\right)
\end{aligned} \tag{20}$$

provides a global upper bound $g(\mathbf{x},\mathbf{y})$ that agrees with $g(\cdot)$ at $\left(x^{(\kappa)},y^{(\kappa)}\right)$, i.e.,

$$g\left(x^{(\kappa)},y^{(\kappa)}\right)=g^{(\kappa)}\left(x^{(\kappa)},y^{(\kappa)}\right), \tag{21}$$

$$g(\mathbf{x},\mathbf{y})\le g^{(\kappa)}(\mathbf{x},\mathbf{y}),\ \forall(\mathbf{x},\mathbf{y}). \tag{22}$$

Next, we use the following concave lower bound for the concave function $f(\mathbf{x},\mathbf{y})$. By property **(P2)**, we have that

$$\begin{aligned}
\ln(1+a_i\mathbf{x}_i+\gamma_{\mathsf{LI},i}\mathbf{y}_i) &\ge \ln\left(1+a_i x_i^{(\kappa)}+\gamma_{\mathsf{LI},i}y_i^{(\kappa)}\right) \\
&\quad + p_i^{(\kappa)}\left(\ln(1+a_i\mathbf{x}_i)-\ln\left(1+a_i x_i^{(\kappa)}\right)\right) \\
&\quad + q_i^{(\kappa)}\left(\ln\mathbf{y}_i-\ln y_i^{(\kappa)}\right),
\end{aligned}$$

$$\ln(1+b_i\mathbf{y}_i)\ge\ln(1+b_i y_i^{(\kappa)})+r_i^{(\kappa)}\left(\ln\mathbf{y}_i-\ln y_i^{(\kappa)}\right),$$

where

$$p_i^{(\kappa)}\triangleq\frac{1+a_i x_i^{(\kappa)}}{1+a_i x_i^{(\kappa)}+\gamma_{\mathsf{LI},i}y_i^{(\kappa)}};\ q_i^{(\kappa)}\triangleq\frac{\gamma_{\mathsf{LI},i}y_i^{(\kappa)}}{1+a_i x_i^{(\kappa)}+\gamma_{\mathsf{LI},i}y_i^{(\kappa)}};$$
$$r_i^{(\kappa)}\triangleq\frac{b_i y_i^{(\kappa)}}{1+b_i y_i^{(\kappa)}}.$$

As such, $f(\mathbf{x},\mathbf{y})\ge f^{(\kappa)}(\mathbf{x},\mathbf{y})$ for

$$\begin{aligned}
&f^{(\kappa)}(\mathbf{x},\mathbf{y})\triangleq \\
&f\left(x^{(\kappa)},y^{(\kappa)}\right)+\sum_{i=1}^{M}\left[p_i^{(\kappa)}\left(\ln(1+a_i\mathbf{x}_i)-\ln(1+a_i x_i^{(\kappa)})\right)\right. \\
&\left.+q_i^{(\kappa)}\left(\ln\mathbf{y}_i-\ln y_i^{(\kappa)}\right)+r_i^{(\kappa)}\left(\ln\mathbf{y}_i-\ln y_i^{(\kappa)}\right)\right].
\end{aligned} \tag{23}$$

Initialized by a feasible solution $\left(x^{(0)},y^{(0)}\right)$ to problem (18), we generate a feasible solution $\left(x^{(\kappa+1)},y^{(\kappa+1)}\right)$ at κ-iteration for $\kappa=0,1,\ldots,$ as the optimal solution of the following convex program:

$$\max_{(\mathbf{x},\mathbf{y})} F^{(\kappa)}(\mathbf{x},\mathbf{y})\triangleq\left[f^{(\kappa)}(\mathbf{x},\mathbf{y})-g^{(\kappa)}(\mathbf{x},\mathbf{y})\right] \quad \text{s.t.}\quad (13)/(14). \tag{24}$$

The concave function $F^{(\kappa)}(\cdot)$ in problem (24) possesses the following two crucial properties:

- It agrees with the nonconcave objective function $F(\cdot)$ at $\left(x^{(\kappa)},y^{(\kappa)}\right)$, i.e.,

$$F^{(\kappa)}\left(x^{(\kappa)},y^{(\kappa)}\right)=F\left(x^{(\kappa)},y^{(\kappa)}\right). \tag{25}$$

- It is a *global lower bound* of the nonconcave objective function $F(\cdot)$, i.e.,

$$F^{(\kappa)}(\mathbf{x},\mathbf{y})\le F(\mathbf{x},\mathbf{y}),\ \forall(\mathbf{x},\mathbf{y}). \tag{26}$$

These two properties guarantee that $F^{(\kappa)}(\cdot)$ is both a local and a global concave approximation of $F(\cdot)$ at $\left(x^{(\kappa)},y^{(\kappa)}\right)$. A proximity control is therefore not necessary.

The convex program (24) provides an iterative *minorant maximization* for nonconvex program (18). Since $(x^{(\kappa)},y^{(\kappa)})$ is feasible to problem (24) itself, it follows that

$$\begin{aligned}
F\left(x^{(\kappa)},y^{(\kappa)}\right)=F^{(\kappa)}\left(x^{(\kappa)},y^{(\kappa)}\right)&<F^{(\kappa)}\left(x^{(\kappa+1)},y^{(\kappa+1)}\right) \\
&\le F\left(x^{(\kappa+1)},y^{(\kappa+1)}\right)
\end{aligned} \tag{27}$$

as long as $\left(x^{(\kappa+1)},y^{(\kappa+1)}\right)\neq\left(x^{(\kappa)},y^{(\kappa)}\right)$. In other words, $\left(x^{(\kappa+1)},y^{(\kappa+1)}\right)$ is a better solution of the nonconvex program (18) than $\left(x^{(\kappa)},y^{(\kappa)}\right)$. Moreover, the necessary optimality condition for $\left(x^{(\kappa)},y^{(\kappa)}\right)$ is $\left(x^{(\kappa+1)},y^{(\kappa+1)}\right)=\left(x^{(\kappa)},y^{(\kappa)}\right)$. That is, for $\left(x^{(\kappa)},y^{(\kappa)}\right)$ to be an optimal solution of the nonconvex program (18), it is necessary that $\left(x^{(\kappa)},y^{(\kappa)}\right)$ is a globally optimal solution of the convex program (24).

Proposition 1 ([8], [15], [16]): For any function $F^{(\kappa)}(\cdot)$ satisfying the agreement condition (25) and the lower bounding condition (26), $\left\{\left(x^{(\kappa)},y^{(\kappa)}\right)\right\}$ is a sequence of improved points, which converges to at least a locally optimal solution of problem (18). Given a tolerance ϵ, the above iterations are finite under the stopping criterion

$$F\left(x^{(\kappa+1)},y^{(\kappa+1)}\right)-F\left(x^{(\kappa)},y^{(\kappa)}\right)<\epsilon. \tag{28}$$

The computational efficiency is therefore is hinges upon the computational tractability of the convex program (24), which boils down to the following convex program:

$$\begin{aligned}
\max_{(\mathbf{x},\mathbf{y})}\ &\sum_{i=1}^{M}\left[p_i^{(\kappa)}\ln(1+a_i\mathbf{x}_i)+\left(q_i^{(\kappa)}+r_i^{(\kappa)}\right)\ln\mathbf{y}_i\right. \\
&\left.-c_i^{(\kappa)}\left(a_i\mathbf{x}_i+(b_i+\gamma_{\mathsf{LI},i})\mathbf{y}_i+\gamma_{\mathsf{LI},i}b_i\mathbf{y}_i^2\right)\right] \\
\text{s.t. }&(13)/(14).
\end{aligned} \tag{29}$$

In the case of power constraint (13), the KKT conditions for necessary and sufficient optimality are:

$$\frac{a_i p_i^{(\kappa)}}{1+a_i\mathbf{x}_i}-c_i^{(\kappa)}a_i+\lambda_{1i}=\lambda, \tag{30}$$

$$\lambda\left(\sum_{i=1}^{M}(\mathbf{x}_i+\mathbf{y}_i)-P\right)=0, \tag{31}$$

$$\frac{q_i^{(\kappa)}+r_i^{(\kappa)}}{\mathbf{y}_i}-c_i^{(\kappa)}\left[(b_i+\gamma_{\mathsf{LI},i})+2\gamma_{\mathsf{LI},i}b_i\mathbf{y}_i\right]+\lambda_{2i}=\lambda, \tag{32}$$

$$\lambda_{1i}\mathbf{x}_i=0,\ \lambda_{2i}\mathbf{y}_i=0,\ \lambda_{1i}\ge0,\ \lambda_{2i}\ge0,\ \lambda\ge0 \tag{33}$$

for $i=1,\ldots,M$. The optimal solution $\left(x^{(\kappa+1)},y^{(\kappa+1)}\right)$ of problem (24) s.t. (13) is then derived as:

$$x_i^{(\kappa+1)}=\max\left\{\frac{p_i^{(\kappa)}}{c_i^{(\kappa)}a_i+\lambda}-\frac{1}{a_i},0\right\}, \tag{34}$$

$$\begin{aligned}
y_i^{(\kappa+1)}&=2\left(q_i^{(\kappa)}+r_i^{(\kappa)}\right)\times\left(c_i^{(\kappa)}(b_i+\gamma_{\mathsf{LI},i})+\lambda\right. \\
&\left.+\sqrt{\left(c_i^{(\kappa)}(b_i+\gamma_{\mathsf{LI},i})+\lambda\right)^2+8\left(q_i^{(\kappa)}+r_i^{(\kappa)}\right)c_i^{(\kappa)}\gamma_{\mathsf{LI},i}b_i}\right)^{-1},
\end{aligned} \tag{35}$$

where $\lambda > 0$ is chosen such that $\left(x^{(\kappa+1)}, y^{(\kappa+1)}\right)$ meets the power constraint (13) with equality. A bisection search can be used to find λ where the initial values are set as $\lambda_{\text{lo}} = 0$ and

$$\lambda_{\text{hi}} = \max_{i=1,\ldots,M} \left\{ \frac{p_i^{(\kappa)}}{P/(3M) + 1/a_i} - c_i^{(\kappa)} a_i, \right.$$
$$\left. \frac{6M}{P}\left(q_i^{(\kappa)} + r_i^{(\kappa)}\right) - c_i^{(\kappa)}(b_i + \gamma_{\text{LI},i}) \right\}.$$

Analogously, in the case of the power constraints (14), the optimal solution of problem (24) s.t. (14) is derived as:

$$x_i^{(\kappa+1)} = \max\left\{ \frac{p_i^{(\kappa)}}{c_i^{(\kappa)} a_i + \lambda_1} - \frac{1}{a_i}, 0 \right\}, \tag{36}$$

$$y_i^{(\kappa+1)} = 2\left(q_i^{(\kappa)} + r_i^{(\kappa)}\right) \times \left(c_i^{(\kappa)}(b_i + \gamma_{\text{LI},i}) + \lambda_2 \right.$$
$$\left. + \sqrt{\left(c_i^{(\kappa)}(b_i + \gamma_{\text{LI},i}) + \lambda_2\right)^2 + 8(q_i^{(\kappa)} + r_i^{(\kappa)}) c_i^{(\kappa)} \gamma_{\text{LI},i} b_i} \right)^{-1}, \tag{37}$$

where $\lambda_1 > 0$ is chosen such that $\sum_{i=1}^M x_i^{(\kappa+1)} = P_1$, and $\lambda_2 = 0$ if $\sum_{i=1}^M y_i^{(\kappa+1)} \le P_2$ at $\lambda_2 = 0$, otherwise $\lambda_2 > 0$ is chosen such that $\sum_{i=1}^M y_i^{(\kappa+1)} = P_2$. A bisection search can be used where the initial values are set as $\lambda_{1,\text{lo}} = \lambda_{2,\text{lo}} = 0$,

$$\lambda_{1,\text{hi}} = \max_{i=1,\ldots,M} \left\{ \frac{p_i^{(\kappa)}}{P_1/M + 1/a_i} - c_i^{(\kappa)} a_i \right\},$$
$$\lambda_{2,\text{hi}} = \max_{i=1,\ldots,M} \left\{ \frac{2M}{P_2}\left(q_i^{(\kappa)} + r_i^{(\kappa)}\right) - c_i^{(\kappa)}(b_i + \gamma_{\text{LI},i}) \right\}.$$

Finally, the proposed iterative water filling algorithm that solves problems (12) s.t. (13)/(14) is summarized as follows.

ALGORITHM 1. *Initialized by a feasible solution* $\left(x^{(0)}, y^{(0)}\right)$ *to problems (12) s.t. (13)/(14), we generate a feasible solution* $\left(x^{(\kappa+1)}, y^{(\kappa+1)}\right)$ *at* κ*-iteration for* $\kappa = 0, 1, \ldots,$ *according to formulae (34)-(35)/(36)-(37).*

Proposition 2: Initialized from a feasible solution $\left(x^{(0)}, y^{(0)}\right)$ to problems (12) s.t. (13)/(14), the sequence of improved solutions $\left\{\left(x^{(\kappa)}, y^{(\kappa)}\right)\right\}$ generated by Algorithm 1 converges to an optimal solution of problems (12) s.t. (13)/(14).

Remark 1: If the HD relaying strategy is used, $\gamma_{\text{LI},i} = 0$ and thus $\gamma(\mathbf{x}_i, \mathbf{y}_i) = \mathbf{x}_i$. We then have the following instantaneous sum-rate maximization per time slot:

$$\max_{(\mathbf{x},\mathbf{y})} \frac{1}{2} \sum_{i=1}^M \ln\left(1 + \frac{a_i \mathbf{x}_i b_i \mathbf{y}_i}{1 + a_i \mathbf{x}_i + b_i \mathbf{y}_i}\right) \tag{38}$$

subject to constraint (13) or (14). Here, the pre-log factor of $1/2$ accounts for the two time slots needed to transmit one data packet. Algorithm 1 can solve problem (38) by letting $\gamma_{\text{LI},i} = 0$ and using (38) to compute the achieved throughput. Such HD throughput can be used as a benchmark for performance comparison with the FD relaying strategy.

IV. Numerical Results

We consider a two-hop relaying network in Fig. 1. Since the two users and the relay are collocated on a line, $d_{S,D} = d_{S,R} + d_{R,D}$. We set the number of antennas as $N = 4$. For each spatial channel, the following pathloss model is used [17]:

$$PL_{dB} = 38 + 30\log_{10}(d) + \psi, \tag{39}$$

where d (in meters) is the transmitter-receiver distance and ψ (in dB) is a correction factor (e.g., to model the outdoor wall penetration loss). We model the shadowing effect by a log-normal random variable with mean of zero and standard deviation of 6dB. To simulate the effect of frequency selectivity in each spatial channel, we assume an exponential power delay profile (PDP) with a root-mean-square (RMS) delay spread of $\sigma_{\text{RMS}} = 3T_s$ where T_s is a constant. The spatial correlation among the MIMO channels is taken from Case B of the 3GPP I-METRA MIMO channel model [18, p.94].

The time-domain channels are converted to the frequency domain by the Fast Fourier transform (FFT) for the computation of the OFDM throughput. We use $K = 1,024$ OFDM subcarriers, each of which occupies a bandwidth of $\Delta f = 15$kHz. Since we take $T_s = 1/(K\Delta f)$, Δf is much smaller than the channel coherence bandwidth of $0.02/\sigma_{\text{RMS}}$ [19, p.85]. The OFDM subchannels are frequency-flat while there is correlation among the adjacent subchannels. In each subchannel, the

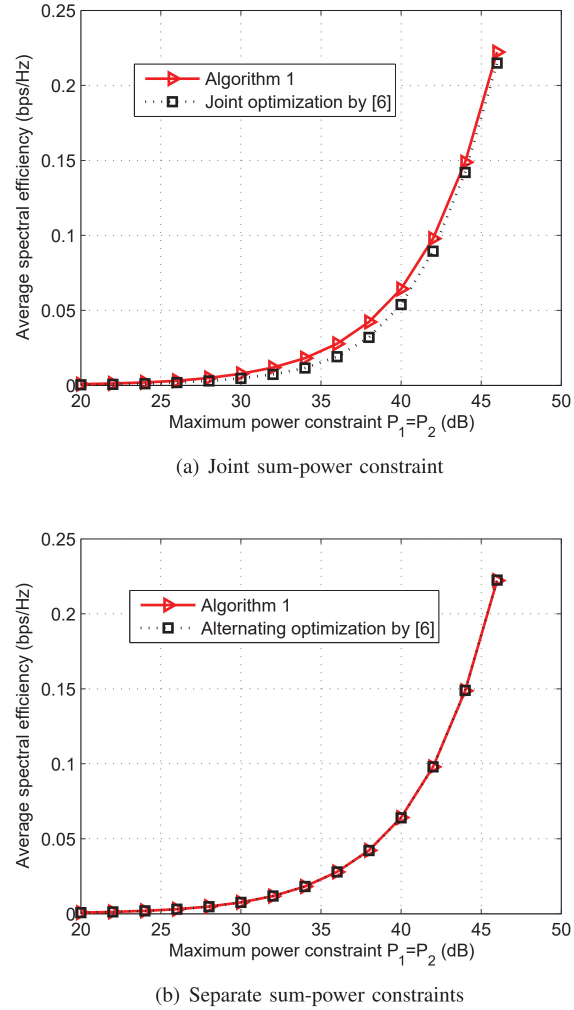

Fig. 2. Throughput comparison with [6] for the HD relaying case

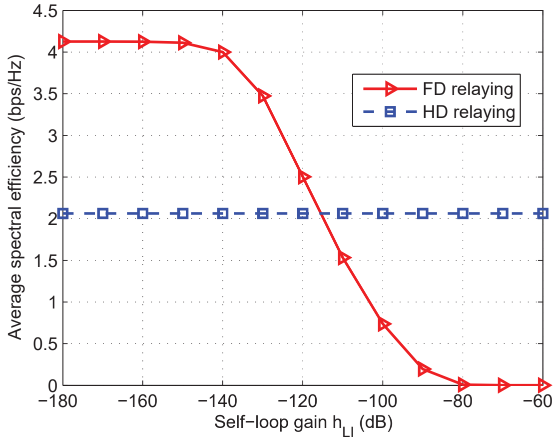

(a) Joint sum-power constraint

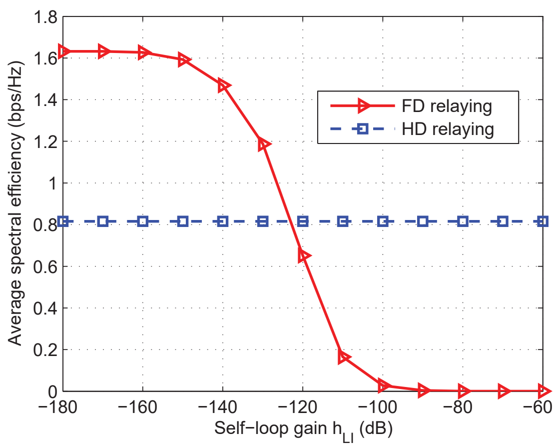

(b) Separate sum-power constraints

Fig. 3. Throughput comparison between FD and HD relaying strategies by Algorithm 1

power spectral density of additive white Gaussian background noise at each antenna is -174dBm/Hz, and the correlation between noise samples from different antennas is 0.2. The effect of all other impairments (including inter-carrier power leakage) is modelled as additive Gaussian noise whose power is twice that of the background noise. For simplicity, we set the self-loop gain as $h_{\mathsf{LI},k,n} = h_{\mathsf{LI}}, \forall i = 1, \ldots, M$. The presented value of h_{LI} is *not* normalized with respect to noise power and $h_{\mathsf{LI}} = 0$ in the HD relaying. We assume $P = P_1 + P_2$ and initialize Algorithm 1 by $x_i = P_1/M$ and $y_i = P_2/M$ for $i = 1, \ldots, M$. We set the error tolerance as $\epsilon = 10^{-4}$, repeat the simulation for 100 independent runs and average the results to get the final figures for spectral efficiency.

First, we compare Algorithm 1 with the two approaches of [6], namely, joint optimization with the high SNR assumption (for the joint sum-power constraint) and alternating optimization (for the separate sum-power constraints). Because the latter solutions only apply to the HD relaying case, we set $\gamma_{\mathsf{LI}} = 0$ in Algorithm 1 for comparison. Here, we set $d_{S,R} = d_{R,D} = 1,000$m, $\psi = 20$dB and assume that each tap of the PDP follows the Rayleigh distribution. Fig. 2(a) verifies that the high SNR approximation is not effective in the low-to-medium SNR scenario that we have simulated. This is demonstrated by the performance gap between the solution of [6] and our proposed solution. Fig. 2(b) shows that Algorithm 1 performs as well as the alternating optimization of [6] for separate sum-power constraints. However, it should be recalled that the alternating optimization approach cannot be used for the joint sum-power constraint case.

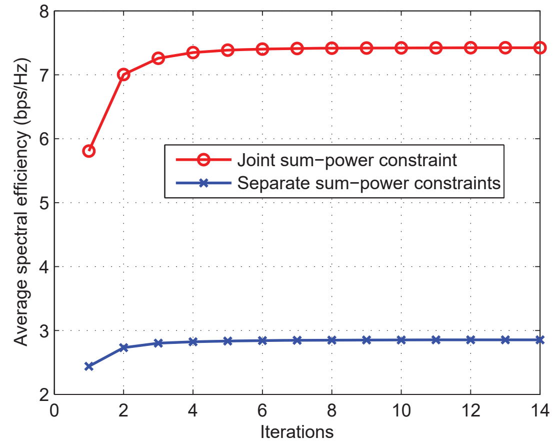

Fig. 4. Convergence of Algorithm 1 for the FD relaying case

To compare FD relaying with HD relaying, we now set $d_{S,R} = d_{R,D} = 500$m, $\psi = 0$dB, $P_1 = 20$dBm and $P_2 = 40$dBm. We assume that each tap of the corresponding channel PDP follows the Rayleigh distribution. From Fig. 3, the achieved throughput by FD almost doubles that by HD at low values of h_{LI}. However, the throughput declines as h_{LI} increases, confirming the intuition that the self-loop interference at the FD relay is the limiting parameter for FD transmissions to be beneficial. Particularly, the gain provided by FD vanishes beyond $h_{\mathsf{LI}} = -120$dB, i.e., it benefits more to stay with the HD transmission beyond this point.

Fig. 4 illustrates the convergence of Algorithm 1 for a random channel realization in the above FD relaying scenario with $h_{\mathsf{LI}} = -140$dB. It is observed that convergence occurs within six iterations at a rather strict error tolerance $\epsilon = 10^{-4}$. Note that each iteration corresponds to evaluating a simple closed-form expression for the solution of a convex program, thus requiring a very little computational effort. Together with the small number of iterations, the total computational complexity is low even for our large-scale numerical examples with $4,096$ subchannels.

V. Conclusions

This paper proposes a large-scale low-complexity algorithm for joint optimal power allocation in a two-hop FD relaying MIMO-OFDM network. The total network throughput is maximized, subject to either the joint sum-power constraint or the separate sum-power constraints at source and relay nodes. To solve the nonconvex formulated problems, the successive convex optimization approach is employed. A simple closed-form solution is available for the approximated convex program in each iteration. The proposed algorithm is shown to always converge to at least a local optimum. The advantages of our novel solutions have been confirmed by numerical examples.

References

[1] Y.-S. Choi and H. Shirani-Mehr, "Simultaneous transmission and reception: algorithms, design and system level performance," *IEEE Trans. Wireless Commun.*, vol. 12, no. 12, pp. 5992–6010, Dec. 2013.

[2] S. Hong, J. Brand, J. I. Choi, J. Mehlman, S. Katti, and P. Levis, "Application of self-interference cancellation in 5G and beyond," *IEEE Commun. Magazine*, vol. 52, no. 2, pp. 114–21, Feb. 2014.

[3] E. Everett, A. Sahai, and A. Sabharwal, "Passive self-interference suppression for full-duplex infrastructure nodes," *IEEE Trans. Wireless Commun.*, vol. 13, no. 2, pp. 680–694, Feb. 2014.

[4] V. Syrjala, M. Valkama, L. Anttila, T. Riihonen, and D. Korpi, "Analysis of oscillator phase-noise effects on self-interference cancellation in full-duplex OFDM radio trancseivers," *IEEE Trans. Wireless Commun.*, vol. 13, no. 6, pp. 2977–2990, Jun. 2014.

[5] W. Li and R. D. Murch, "An investigation into baseband techniques for single-channel full duplex wireless communication systems," *IEEE Trans. Wireless Commun.*, vol. 13, no. 9, pp. 4794–4806, Sep. 2014.

[6] I. Hammerstrom and A. Wittneben, "Power allocation schemes for amplify-and-forward MIMO-OFDM relay links," *IEEE Trans. Wireless Commun.*, vol. 6, no. 8, pp. 2798–2802, Aug. 2007.

[7] D. W. K. Ng, E. S. Lo, and R. Schober, "Dynamic resource allocation in MIMO-OFDMA systems with full-duplex and hybrid relaying," *IEEE Trans. Commun.*, vol. 60, no. 5, pp. 1291–1303, May 2012.

[8] H. H. Kha, H. D. Tuan, and H. H. Nguyen, "Fast global optimal power allocation in wireless networks by local d.c. programming," *IEEE Trans. Wireless Commun.*, vol. 11, pp. 511–515, Feb. 2012.

[9] ——, "Joint optimization of source power allocation and cooperative beamforming for SC-FDMA multi-user multi-relay networks," *IEEE Trans. Commun.*, vol. 61, no. 6, pp. 2248–2259, Jun. 2013.

[10] O. Edfors, M. Sandell, J.-J. van de Berek, S. K. Wilson, and P. O. Borjesson, "OFDM channel estimation by singular value decomposition," *IEEE Trans. Commun.*, vol. 46, no. 7, pp. 931–939, Jul. 1998.

[11] B. P. Day, A. R. Margetts, D. W. Bliss, and P. Schiniter, "Full-duplex bidirectional MIMO: achievable rate under limited dynamic range," *IEEE Trans. Signal Process.*, vol. 60, no. 7, pp. 3702–3713, Jul. 2012.

[12] ——, "Full-duplex MIMO relaying: achievable rate under limited dynamic range," *IEEE J. Select. Areas in Commun.*, vol. 30, no. 8, pp. 1541–1553, Sep. 2012.

[13] M. Duarte, A. Sabharwal, V. Aggarwal, R. Jana, K. Ramakrishnan, C. Rice, and N. Shankaranarayanan, "Design and characterization of a full-duplex multiantenna system for WiFi networks," *IEEE Trans. Veh. Technol.*, vol. 63, no. 3, pp. 1160–1177, Mar. 2014.

[14] J. Papandriopoulos and J. S. Evans, "SCALE: a low-complexity distributed protocal for spectrum balancing in multi-user DSL networks," *IEEE Trans. Inform. Theory*, vol. 55, no. 8, pp. 3711–3724, Aug. 2009.

[15] P. Apkarian and H. D. Tuan, "Concave programming in control theory," *J. of Global Optimization*, vol. 15, pp. 243–270, Apr. 1999.

[16] ——, "Robust control via concave optimization: local and global algorithms," *IEEE Trans. Automatic Control*, vol. 45, no. 2, pp. 299–305, Feb. 2000.

[17] European Telecommunications Standards Institute (ETSI), "3GPP TR 36.931, version 9.0.0, Release 9," Tech. Rep., May 2011.

[18] Y. S. Cho, J. Kim, W. Y. Yang, and C. G. Kang, *MIMO-OFDM Wireless Communications with MATLAB*. Wiley-IEEE Press, Aug. 2010.

[19] A. Goldsmith, *Wireless Communications*. Cambridge University Press, 2004.